Atmos. Chem. Phys. Discuss., https://doi.org/10.5194/acp-2017-544
Manuscript under review for journal Atmos. Chem. Phys.
Discussion started: 22 June 2017

Atmospheric Chemistry and Physics Discussions

Long-range isentropic transport of stratospheric aerosols over Southern Hemisphere following the Calbuco eruption in April 2015

Nelson. Bègue[1], Damien. Vignelles[2], Gwenaël. Berthet[2], Thierry. Portafaix[1], Guillaume. Payen[1], Fabrice. Jégou[2], Hassan. Benchérif[2,6], Julien. Jumelet[3], Jean-Paul Vernier[4], Thibaut. Lurton[2], Jean-Baptiste. Renard[2], Lieven. Clarisse[5], Vincent. Duverger[2], Françoise. Posny[1] Jean-Marc. Metzger[1] and Sophie. Godin-Beekmann[3]

[1] Laboratoire de l'Atmosphère et des Cyclones, UMR 8105 CNRS, Université de la Réunion, Reunion Island, France.

[2] Laboratoire de Physique et Chimie de l'Environnement et de l'Espace, Université d'Orléans, CNRS/INSU UMR7328, Orléans, France

[3] Laboratoire Atmosphère Milieux Observations Spatiales, University of Paris VI, Paris, France

[4] NASA Langley Research Center, Hampton, Virginia, USA

[5] Spectroscopie de l'Atmosphère, Service de Chimie Quantique et Photophysique, Université Libre de Bruxelles, Brussels, Belgium

[6] School of Chemistry and Physics, University of KwaZulu-Natal, Westville, Durban, South Africa

Correspondence to: N.Bègue (nelson.begue@univ-reunion.fr)

Abstract

After 43 years of inactivity, the Calbuco volcano which is located in the southern part of Chile erupted on 22 April 2015. The space-time evolutions (distribution and transport) of its aerosol plume are investigated by combining satellite (CALIOP, IASI, OMPS), in situ aerosol counting (LOAC OPC) and lidar observations, and the MIMOSA advection model. The Calbuco aerosol plume reached the Indian Ocean 1 week after the eruption. Over the Reunion Island site (21°S; 55.5°E), the aerosol signal was unambiguously enhanced in comparison with "background" conditions with a volcanic aerosol layer extending from 18 km to 21 km during the May-July period. All the data reveal an increase by a factor of ~2 in the SAOD (Stratospheric Aerosol Optical Depth) with respect to values observed before the eruption.

Atmos. Chem. Phys. Discuss., https://doi.org/10.5194/acp-2017-544
Manuscript under review for journal Atmos. Chem. Phys.
Discussion started: 22 June 2017

Atmospheric Chemistry and Physics Discussions

The aerosol e-folding time is approximately 90 days. Microphysical measurements obtained before, during and after the eruption reflecting the impact of the Calbuco eruption on the lower stratospheric aerosol content have been analyzed over Reunion site. During the passage of the plume, the volcanic aerosol was characterized by an effective radius of 0.16 ±0.02 µm with an unimodal lognormal size distribution and the aerosol number concentration appears 20 times higher than before and one year after the eruption. A tendency toward "background" conditions has been observed about one year after the eruption, by April 2016. The volcanic aerosol plume is advected eastward in the Southern Hemisphere and its latitudinal extent is clearly bounded by the subtropical barrier and the polar vortex. The transient behavior of the aerosol layers observed above Reunion Island between May and July 2015 reflects an inhomogeneous geographical distribution of the plume which is controlled by the latitudinal motion of these dynamical barriers.

1. Introduction

Stratospheric aerosol affect the chemical and radiation balance of the atmosphere (McCormick et al., 1995; Solomon, 1999; SPARC 2006). The importance of stratospheric aerosol on the chemistry is meanly due to their role on ozone budget (Solomon et al., 1986; Bekki, 1997; Borrmann et al., 1997). Indeed, stratospheric aerosol provide sites for heterogeneous chemical reactions leading to stratospheric ozone depletion, significantly enhanced in periods of high aerosol loadings following major volcanic eruptions (Solomon, 1999 and references therein). In addition, periods of enhanced stratospheric aerosol loadings can lead to significant warming in the stratosphere and cooling in the troposphere (e.g. McCormick et al., 1995; Solomon et al., 2011; Arfeuille et al., 2013). As reported by Kremser et al. (2016), a better understanding of the processes governing the lifetime of stratospheric aerosol is needed to assess the impacts on climate and chemistry. Since the discovery of the permanent stratospheric aerosol layer, called Junge Layer, in 1961 (Junge, 1961), it has been established that stratospheric aerosol are mostly composed of sulfuric acid droplets with some more complex characteristics in the lower stratosphere and upper stratosphere where organic compounds and meteoritic dust can also contribute to its composition (Neely et al., 2011, Froyd et al., 2009). The main sources of stratospheric sulfur are Carbonyl Sulfide (OCS), Dimethyl Sulfide (DMS) and sulfur dioxide (SO_2) (SPARC, 2006), the latest being significantly enhanced after volcanic eruptions (Carn et al., 2015). The injected SO_2 is then oxidized into H_2SO_4, which after homogeneous nucleation and/or condensation onto existing aerosol, results in an increase in the content of liquid sulfate aerosol (SPARC, 2006).

Thomason et al. (2007) have shown that volcanic effects have dominated other natural and anthropogenic sources on the control of the stratospheric aerosol burden over the last 25 years. Previous studies on stratospheric aerosol have mainly contributed to characterize their properties and variability during "background" (i.e. free of volcanic aerosol) and volcanic conditions (e.g., Stenchikov et al., 1998; Jäger and Deshler, 2002; Bauman et al., 2003; Hermann et al; 2003; Hofmann et al; 2009).

The eruption of the Pinatubo in 1991 is known to be the last major volcanic eruption which injected up to 20 Tg of SO_2 and perturbed significantly the global stratosphere for several years (Kinninson et al., 1994; McCormick et al., 1995; Stenchikov et al., 1998, 2002; Dhomse et al., 2014). As reported by Russell et al. (1996), in addition to the prodigious increase in the stratospheric aerosol loading, this event has significantly affected numerous aspects of the atmospheric system including: i) a 2-year cooling of the global surface temperature of several tenths of degrees (Canty et al., 2013; Wunderlich and Mitchell, 2017) ii) a warming of the tropical stratosphere (~3,5 K) near the aerosol peak (Labitze and McCormick et al., 1992) or also a lifting of the tropical ozone layer by ~1.8 km (Pueschel et al., 1992; Grant et al., 1994). By the use of satellite and balloon-borne observations, studies have shown that moderate volcanic eruptions (i.e., 10-20 times weaker than Pinatubo eruption in term of injected sulfur) could significantly modulate stratospheric aerosol concentrations (Bourassa et al., 2010; Kravitz et al., 2010; Solomon et al., 2011; Vernier et al., 2011; Clarisse et al., 2012; Jégou et al., 2013). Based upon satellite observations, Vernier et al (2011) showed that the decadal increase in stratospheric aerosol loadings since 2002 can be attributed to a series of moderate volcanic eruption. As reported by Kremser et al (2016), this decadal trend was also obtained from lidar (Hofmann et al., 2009) and ground-based sun-photometer observations (Ridley et al., 2014). Three moderate volcanic eruptions are ranked in the top 10 of the most influential events on the stratospheric aerosol burden including: (1) The Kasatochi eruption (52° N; 175°W, Alaska) in 2008 which injected 1.5-2.5 Tg of SO_2 into the upper troposphere and lower stratosphere (UTLS) (Bourassa et al., 2010; Kravitz et al., 2010; Krotkov et al., 2010); (2) The Sarychev eruption in June 2009 (48.1°N; 153.2°E, Kuril Island) which released 0.9 Tg of SO_2 into the UTLS (Clarisse et al., 2012; Kravitz et al., 2011; Jégou et al., 2013); (3) The Nabro eruption (13°N; 41°E, Eritrea) in June 2011 which emitted 1.3 Tg of SO_2 (Bourassa et al., 2012; Sawamura et al; 2012). In comparison, these recurrent "minor" volcanic eruptions injected 10-20 times less SO_2 than Mt Pinatubo, but contributed to counterbalance the global warming observed between 2000 and 2010 (Solomon et al., 2011). These eruptions can also

be used to understand stratospheric dynamic as it was done after Mt Pinatubo (Trepte et al., 1992).

Indeed, following a volcanic eruption, stratospheric aerosol can be used as dynamical tracers (Bencherif et al., 2003; Fairlie et al., 2014). Based on satellite observations and a lagrangian trajectory model, Fairlie et al. (2014) used the dispersion of the Nabro plume to study the dynamics of the Asian Monsoon Anticyclone. Hitchman et al. (1994) and SPARC (2006) suggested that the stratospheric aerosol distributions could be used to understand changes in the Brewer-Dobson Circulation. Previous works have also revealed that stratospheric aerosol can be used to study meridional transport from the tropical stratospheric reservoir (Trepte and Hitchman, 1992; Randel et al., 1993; Chen et al., 1994; Grant et al., 1996, Vernier et al., 2009). Based on satellite observations, Trepte and Hitchman (1992) have shown that transport to mid-latitudes is mainly favored during westerly shear phases of the QBO than during the easterly shear phases. More recently, by the use of satellite observations and climate models, Hommel et al. (2015) revealed that the vertical and latitudinal extent of the stratospheric aerosol layer (between 16 and 31 km) in the tropics is modulated by QBO.

This paper reports on the Calbuco plume observations over Reunion Island and its transport in the southern tropics. The geometrical and optical properties of the Calbuco plume are inferred from the ground-based observations at Reunion Island in the framework of the MORGANE (Maïdo ObservatoRy Gas Aerosols NDACC Experiment) campaign. The aim of this study is to provide the dynamical framework controlling the time-space evolution of the volcanic plume in the southern hemisphere. The paper is organized as follows: Section 2 describes the observations and the model used for the investigation of the volcanic aerosol transport. A description of the long-range transport of the volcanic plume over the Indian Ocean is provided in Section 3; Section 4 gives a dynamical analysis of this case study; and the summary and the conclusions are given in Section 5.

2. Instrumentation and model description

2.1 Observations

2.1.1 Ground-based lidar

One part of the observations used in this study was performed during the MORGANE campaign which took place at the Maïdo observatory on Reunion Island (21°S; 55°E) in May 2015. The MORGANE ground-based observational systems combine Lidar and balloon-borne payloads to study the composition and the dynamics of the Upper Troposphere-Lower

Stratosphere (UTLS) in the southern hemisphere. Among the 4 lidar systems operated during this campaign, we used the measurements from the stratospheric DIfferential Absorption Lidar (DIAL) system built for the monitoring of the stratospheric ozone profile (Baray et al., 2013). It is possible to retrieve also aerosol profiles in the 15-38 km altitude range from these measurements. This instrument has been in operation at the Maïdo observatory since early 2013. The technical details and evaluation of its performance are given by Baray et al., (2013). A brief description of this DIAL system is given hereafter. It uses a tripled Nd:YAG laser which provides a beam at 355 nm wavelength with a repetition rate of 30 Hz and a XeCl excimer laser which emits a radiation at 308 nm at 40 Hz. The optical receiver is a telescope composed of 4 parabolic mirrors where the backscattered signal is collected by 4 optical fibers located at the focal points. The current configuration of the DIAL lidar system mainly detects in the UV bands (308, 332, 355 and 387 nm). The lidar data set used in this study consists of daily records of backscattering signal obtained from the Maido facility between 1 November 2014 and 30 November 2016 (106 profiles). It should be noted that no measurements were recorded at Reunion from January to April 2016 because of technical problems. The daily measurements are nocturnal and time-integrated over about 3 hours in average.

The method involves obtaining the extinction and backscatter coefficient from a Rayleigh Mie lidar has been described first by Klett (1981). The methodology of Sasano (1985), used here, is similar and has the advantage to give a numerical calculation of the extinction and backscatter coefficient. Several parameters are needed: first, the temperature and the pressure come from a radiosounding realized in the airport of Gilot at 11h (UTC). The profile is completed by the Arletty model, based on European Centre for Medium Range Weather Forecast (ECMWF) data. The second parameter is the ratio between the backscatter and the extinction coefficient for aerosol, also call lidar coefficient. It depends of the kind of aerosol. In the case of background stratospheric aerosol, the value found in the literature is near 60. The third parameter is the altitude of reference defined as the altitude where there is no aerosol. The altitude of reference is determined for each profile. On average, the altitude of reference is located between 30 and 40 km.

2.1.2 Balloon-borne OPC.

In order to analyze the concentration and the size of the observed aerosol over the site, many LOAC (Light Optical Aerosols Counter) systems were launched together with balloon-ozonesondes. A detailed description of the LOAC is given by Renard et al. (2016). In brief,

LOAC is a lightweight Optical Particle Counter (OPC) of 1 kg which can fly under latex weather balloons. Through the measurements of the light scattered by particles at two specific angles (Lurton et al. 2014), it provides aerosol concentrations and particle size distributions for 19 size classes ranging from 0.2 µm to 50 µm in diameter every ten seconds with a vertical resolution of nearly 50 m depending on the ascent rate of the balloon. The number concentration range is from 0.6 to a few thousands particles per cm^3 (Vignelles 2017). Uncertainties on number concentration during the ascent under meteorological balloon are mainly due to temperature variation effects on electronics (Renard et al. 2016, Vignelles 2017). Uncertainties on number concentrations for size bins than 1 µm is estimated to be of ± 30 %. For larger size bins, uncertainties on number concentration is dominated by Poisson law statistics estimated to be ± 20 % and ± 60 % at concentrations respectively lower than 10^{-1} and 10^{-2} part per cm^3.

2.1.3 CALIOP

The Cloud-Aerosols Lidar with Orthogonal Polarization (CALIOP) on board The Cloud-Aerosols Lidar and Infrared Pathfinder Satellite Observation (CALIPSO) was used to study the transport of the Calbuco plume. CALIPSO was launched in 2006 to a Sun-synchronous polar orbit (Winkler et al., 2007) with a repeat cycle of 16 days. CALIPSO is composed of an Infrared Imager Radiometer (IIR), a wide field visible camera and the CALIOP lidar. CALIOP is a two-wavelength polarization-sensitive lidar (532 and 1064 nm) which measures total attenuated backscatter vertical profiles with altitude-varying vertical (30-300 m) and horizontal (300-5000 m) resolution (Winker et al., 2010). The data used in this study are the total and perpendicular backscatter coefficient at 532 nm available from the CALIOP level 1B V4.01 product. These data have been averaged every 1 degree in latitude for each orbit and grouped into data files containing 16 days of measurements. From there, Scattering Ratio and Depolarization Ratio coefficients at 532 nm have been calculated (Vernier et al., 2009). Through the use of this algorithm, the full zonal mean between 20°S and 20°N are obtained by averaging 7200 cells, leading to a precision of ± 1.6 % (Vernier et al., 2009). The ability of CALIOP to detect small volcanic plumes in the lower tropical stratosphere has been highlighted in previous studies (Thomason et al., 2007; Vernier et al., 2009, 2011).

2.1.4 IASI

The Infrared Atmospheric Sounding Interferometer (IASI) observations were used to quantify the amount of SO_2 emitted during the Calbuco eruption. IASI is a nadir looking thermal

infrared sounder on board the Meteorological Operational satellite (MetOp-A and MetOp-B) launched in October 2006 with a polar orbit. Its global spatial coverage and its footprint of 12 km make IASI relevant for monitoring of the key atmospheric species, in particular for the volcanic SO_2 (Clarisse et al., 2008, 2012; Clerbaux et al., 2009). The amount and altitude of emitted SO_2 were obtained from the algorithms detailed in Clarisse et al. (2012) and Clarisse et al. (2014) respectively. For each IASI observation, the height was estimated first, after which the column was calculated using the height information as an input parameter. In this study, only data from MetOp-A was used.

2.1.5 OMPS

The Ozone Mapper and Profiler Suite (OMPS) Limb Profiler (LP) is also used in the present study to analyze the optical properties of the volcanic plume over the Reunion site. OMPS was launched on October 2011 on board the Suomi National Polar Partnership (NPP) spacecraft. The data used in this study are the daily extinction profiles at 675 nm. A detailed description of the aerosol extinction retrieval algorithm is given by Jaross et al. (2012) and Rault and Loughman (2013). Briefly, the measured spectrum is used to infer information on the size distributions and the radiances are normalized to their value at 35.5 km (weak contribution of aerosol extinction). Then, the extinction coefficients are retrieved using the Rodgers' maximum likelihood technique**.** We used 2 years (From November 2014 to November 2016) of satellite overpasses above the lidar site, within a 5°x5° in latitude and longitude grid. OMPS data have already used to be very effective at detecting and characterizing major events, such as the Chelyabinsk bolide in February 2013 (Gorkavyi et al., 2013).

2.2 MIMOSA model

The Modèle Isentropique de transport Mésoéchelle de l'Ozone Stratosphérique par Advection (MIMOSA) model (Hauchecorne et al., 2002) is a Potential Vorticity (PV) advection model running on isentropic surfaces. The advection scheme is semi-Lagrangian with a time step of 1 hour. The re-gridding onto the original orthonormal grid is performed every 6 hours. The model resolution is 0.5°x0.5°. The advection is driven by ECMWF meteorological analyses at a resolution of 0.5°x0.5°. In the case of the PV, its slow diabatic evolution is taken into account by relaxing the model PV towards the PV calculated from the ECMWF fields with a relaxation time of 10 days. Using this procedure, it is possible to run the model continuously and follow the evolution of PV filaments during several months. The accuracy of the model

has been evaluated by Hauchecorne et al. (2002) and validated against airborne lidar ozone measurements using correlation between PV and ozone, a quasi-conserved chemical tracer on a week timescale within most of lower stratosphere (Heese et al., 2001).

2.3 DyBAL code

The Dynamical BArrier Location (DyBAL) code is an original software developed at the Laboratoire de l'Atmosphere et des Cyclones (LACy, France) to detect the subtropical barrier position (Portafaix et al., 2003). The dynamical barriers are detected from the equivalent length of the tracer contour and the gradient of isentropic Ertel's potential vorticity (PV) in equivalent latitude coordinate as defined by Nakamura (1996). These two diagnostic tools are used by DyBAL to identify weak mixing and transport barriers. The position of the dynamical barrier is characterized by a local maximum of the PV gradient and a local minimum of the equivalent length (Nakamura, 1996). The DyBAL code is applied to the PV map obtained from the MIMOSA model runs. The ability of DyBAL to detect the position and the deformation of the dynamical barriers has been highlighted in previous studies (Bencherif et al., 2007; Morel et al., 2005; Portafaix et al., 2003).

3. Long-range transport and evolution of the Calbuco volcanic plume over the Indian Ocean

3.1 Formation and transport

3.1.1 SO_2 plume

After 43 years of inactivity, the Calbuco erupted on 22 April 2015 and two intense explosive events were recorded during the same week. Figure 1 shows the CALIOP cross-section of the 532nm total attenuated backscatter (ATB) for the overpass over South America on 24 April. The ATB signals ranging from 1 10^{-3} to 5 10^{-3} km^{-1} sr^{-1} correspond to weak values of brightness temperatures over the southern part of Brazil (34, 22°S; 53, 97°W) can be attributed to volcanic material injected up to the lower stratosphere by the Calbuco eruption.

The evolution of the SO_2 total mass measured by IAI between 23 April 2015 and 31 May 2015 is reported in Figure 2. The SO_2 total mass is defined as the sum of SO_2 mass over the atmospheric column from midday to midnight over the southern hemisphere. As expected an increase of the SO_2 amounts was observed by IASI a few days following the Calbuco eruption. One day after the eruption the SO_2 total mass was 10 times higher than background levels. The SO_2 total mass increased quickly to its maximum value (0.41 Tg) on 25 April

2015 and slowly decreased to reach values close to the background values on 19 May 2015 (Figure 2). An e-folding times of ~11 days can be estimated which is in agreement with the value reported for the Sarychev volcanic eruption (Jégou et al., 2013). The SO_2 total mass increased again on 28 May 2015 to reach a secondary maximum (0.13 Tg) on 30 May 2015. This new increase of the SO_2 total mass could be due to the Wolf eruption (Isabela Island, Galapagos) which occurred on 25 May 2015 (Xu et al., 2016). The amount of SO_2 emitted during the Calbuco eruption is about two times lower than the SO_2 mass emitted from the Sarychev eruption in June 2009 (Jégou et al., 2013). It is also worth noting that the SO_2 mass injected during this event is of the same order as quantified during the Grimsvötn eruption in May 2011 (Clarisse et al., 2011). Given that the amount of SO_2 emitted in comparison to previous volcanic eruptions, the Calbuco eruption can be considered as moderate in term of produced aerosol loading. Figure 2 also depicts the maximum altitude of the SO_2 plume over the period from 23 April 2015 to 31 May 2015. On average the maximum of SO_2 is located in the lower stratosphere region around 17 km.

The SO_2 measurements integrated from midday to midnight obtained from IASI are also used to describe the transport of the volcanic plume over the southern hemisphere (Figure 3). On 23 April 2015, part of the plume is present nearby Uruguay coast at 17 km and transported by the general circulation. The plume reached Southern Africa and East side of Madagascar on 1 May 2015 at altitude of 17-18 km and was organized following a cyclonic rolling (Figure 3b). On 6 May, the plume is mainly located over the Atlantic Ocean near the east coast of South Africa and partly over Namibia and South Africa. The SO_2 plume extent and amplitude began to diminish on 11 May 2015 as expected by the oxidation of SO_2 to gaseous sulphuric acid which further condensed into H_2SO_4-H_2O liquid aerosol. The plume was embedded in a thin layer between 15-17 km extending from the Atlantic Ocean to the Indian Ocean passing through the Cape of Good Hope (Fig. 3d).

3.1.2 Spatial extent of the aerosol plume

The transport of the volcanic aerosol plume over the southern hemisphere can be followed by CALIOP observations at 532 nm. Figure 4 presents the latitude-altitude cross sections of the scattering ratio observed by CALIOP for 16-day selected periods in 2015. The scattering ratio values observed during the 16-30 April period (before the eruption) in the Southern hemisphere, particularly in the lower stratosphere, were in average at 1.05 (not shown). Between one and three weeks after the eruption (1-16 May period), CALIOP observations reveal that SR increased until 1.12 in the southern lower stratosphere. The amplitude of the

plume during the first weeks following the eruption was higher than the background aerosol levels at mid-latitudes but was still below the scattering ratio values observed in the tropics. This could be attributed to possible remnants of the Kelud (7.5°S; 112.2°E; erupted in February 2014) volcanic aerosol superimposed to the equatorial background aerosol layer. About one month after the eruption (16-31 May period) the Calbuco plume was much more pronounced with scattering ratio values (ranging from 1.16 to 1.18) largely above background levels and greater than aerosol amounts confined in the tropical reservoir. The plume extended up to about 20 km in altitude and spread over a wide range of latitudes by nearly reaching 60°S and showing a feature of intrusion into low latitudes, i.e. near 5°S. The rough center of the plume was therefore slightly norther than the eruption. About one month later on (16-30 June period), the plume top had moved upward by several hundred meters and was thicker. The southern hemisphere between 10°S and polar latitudes was full of volcanic aerosol with scattering ratio values much higher than elsewhere in the whole stratosphere. About four months after the eruption (16-31 August period) the volcanic aerosol layer was even thicker with scattering ratio remaining high.

In the upper stratospheric transport regime, i.e. in the 21-28 km altitude range, detrainment of aerosol from the equatorial reservoir appears dependent upon the phase of the quasi-biennial oscillation (QBO) and on the intensity of planetary wave activity (Trepte and Hitchman, 1992). When QBO easterlies descend in the tropics, planetary waves are blocked from entering this region, thus limiting the extent to which these waves may have detrained aerosol laterally from the tropical reservoir (Trepte et al., 1993). This corresponds to the situation in Figure 4. However, during the westerly phase of the QBO particles tend to spread poleward and mixing across the subtropics are expectedly favored, especially in winter (Trepte et al., 1993). The meridional spread in aerosols amounts shown above 21 km in Figure 4c and 4d may therefore be consistent with the phase reversal of the QBO from easterlies to westerlies observed from mid-2015.

3.2 Evolution of the aerosols plume over the Reunion site

3.2.1 Ground-based and satellite observations

Figure 5 depicts the evolution of the stratospheric AOD (SAOD) at 532 nm calculated between 17 and 30 km from the Reunion ground-based lidar and OMPS observations over Reunion from November 2014 to November 2016. SAOD were calculated from lidar and OMPS observations at 532 nm using angstrom exponent equal to 1.3 and 1.8 respectively

(Schuster et al., 2006; Jäger and Deshler 2002). As expected, an increase in the aerosol loading was observed over the Reunion site a few weeks after the Calbuco eruption. OMPS data show a doubling in the SAOD record in comparison with values observed at the end of 2014 and at the beginning of 2015 (Fig. 5). SAOD reached its maximum values (0.014 for OMPS) at the beginning of June 2015, decreased afterward to 0.01 on August 2015 and went back to pre-eruption values (0.004-0.006) in April 2016. The lidar record peaks at the same period, but SAOD values are 1.2 times weaker than those observed by OMPS during the June-December period. The lidar SAOD observations show less difference with values obtained prior to the eruption (0.008).Discrepancies between OMPS and lidar were significantly reduced in April 2016, i.e. with relative difference of 25% and 10% over the January-December 2015 period and over the April-November 2016 period respectively. The reasons for these discrepancies are unclear but effects due to different spatial samplings cannot be excluded. From both datasets an aerosol e-folding of approximately 90 days can be derived, which is rather close to the value (~80 days) reported for the Sarychev eruption (Jégou et al., 2013).

Figure 6a illustrates the weekly-averaged extinction profiles at 532 nm derived from lidar measurements over Reunion. This figure reveals a sharp increase of the extinction between 18 and 19 km in May 2015 and reaching its maximum value (greater than 4 10^{-3} km^{-1}) in June. The vertical extent of the plume had increased significantly over the May-July period with a volcanic aerosol layer spanning from 18 to 21 km. At the beginning of June, the plume was structured in two layers with the first one centered at 18.5 km and the second one at 20 km (Fig.6a). We note also a quick decrease in the local extinction around mid-May. The variability observed in the weekly-averaged extinction profiles and in the vertical extent of the aerosol signal over the May-July period reflects the presence of transient aerosol layers above Reunion and indicates that the plume is not homogeneously distributed at this stage. The altitude of the volcanic aerosol plume and the extinction values decreased from mid-August onwards. The plume is hence centered around 18 km on September. Overall, the temporal evolution of the weekly-averaged extinction presents similar general features as the lidar observations, with maximum values in June and a subsequent gradual decrease of the aerosol signal. Nevertheless, in OMPS data the plume is smeared out over a wider vertical range than in the lidar record (Fig. 6b). The vertical and horizontal structures of the plume are not reproduced in OMPS data. In particular, the decrease in the plume altitude in mid-August is not observed by OMPS. This can be due to dilution (along the space borne instrument lines of

sights) of the aerosol signal and vertical resolution issues. The evolution of the scattering ratio at 532 nm obtained from the lidar and CALIOP space-borne observations during the April-December 2015 period over the Reunion site are presented on Figure 7. The scattering ratios from CALIOP have been averaged within ± 5°in latitude and ± 50° in longitude around Reunion Island (Fig. 7b). CALIOP observations confirm also the presence of the volcanic aerosol plume over the Reunion site at the beginning of May 2015 with maximum scattering ratio values (greater than 1.9) on mid-May 2015. Overall, the aerosol variability is smoother in CALIOP observations than in the lidar record, which shows more fluctuations in the altitude of the volcanic plume. Conversely to the lidar and OMPS observations, CALIOP data do not point out an increase of the vertical extent of the plume and maximum scattering ratio values at the beginning of June 2015. According to CALIOP, the scattering ratio begin to decrease at mid-June followed by a slight decrease of the altitude of the plume since the end of July (Fig 7b). From July onwards, the CALIOP aerosol scattering ratio decreases gradually with similar values as observed by the lidar.

3.2.2 In-situ observations

Four LOAC OPCs were launched over the Reunion site from November 2014 to November 2016. SAOD were calculated at 532 nm following Mie Theory. LOAC observations reveal also an increase by a factor of 2 in the SAOD on 19 May 2015 ($1.35\ 10^{-2}$). Then SAOD decrease to $8.4\ 10^{-3}$ on 19 August 2015 followed by a return to pre-eruption levels on November 2016 (Fig. 5). Though the SAOD overall evolution derived from LOAC compares fairly well to OMPS and lidar observations accounting for error bars (Fig. 5), the discrepancies in terms of SAOD amplitude mainly observed in May could be due to the different measurement techniques using different spatial and temporal coverages. The integration time of the LOAC instrument and the ascent velocity of the balloon limit the vertical resolution on the profile. The in situ data are averaged over 1 minute which tends to spread out the structure attributed to the volcanic aerosol plume and can explain the difference with the daily-integrated lidar observations.

Figure 8 illustrates the volume concentration (dN/dln(D)) and number concentration (DV/dln(D)) obtained from the LOAC OPC observations over the Reunion site on 19 May 2015 at 1746 UTC. The best fit obtained from LOAC OPC observations reveals an unimodal lognormal size distribution (Fig. 8). We note that the shape of the size distribution obtained during the Calbuco event is similar to the results obtained by Kravitz et al. (2011) for the Sarychev eruption. As suggested by Kravitz et al. (2011) for the Sarychev event, we can also

assume that the Calbuco eruption did not eject enough material to create a bimodal structure over Reunion Island. The effective radius derived from the LOAC OPC on 19 May is 0.17 ±0.02 µm reflecting that the particles observed several weeks after the Calbuco eruption are quite small. Interestingly, Jégou et al. (2013) have reported that the effective radius obtained during the Sarychev event ranged from 0.15 to 0.20 µm more than one month after the eruption, in agreement with the results of O'Neill et al. (2012). Therefore both eruptions are comparable in terms of size distribution shape and effective radius. Conversely to the Calbuco and Sarychev moderate eruptions, bimodal size distributions were observed for the Pinatubo aerosols on the first weeks after the eruption, the second mode possibly consisting of volcanic ash (e.g. Russell et al., 1996). Russell et al. (1996) have reported that in the month following the Pinatubo eruption the effective radius did not differ greatly from pre-eruption values (i.e. 0.17 ± 0.07 µm in their study) possibly because a large number of particles with sizes both smaller and larger than 0.17 µm were injected.

The integrated number of particles obtained over 19 size classes from 0.2 to 2 µm in diameter is presented in Figure 9. A local aerosol concentration enhancement is detected in the lower stratosphere (16.8-19 km) over Reunion on 19 May 2015 at 1746 UTC. A maximum concentration of about 150 particles per cm^3 (total number of particles: 730 ± 130 particles (±1σ)) is observed by the aerosol counter for particle sizes larger than 0.2 µm. This aerosol number concentration appears 20 times higher than the one observed by the LOAC flight on 26 November 2014 at 1442 UTC. Few in situ observations are available in the tropical region to provide a reference state of the background aerosol content. Based on COPAS measurements (Condensation PArticle counter System, Weigel et al., 2009) on board the M-55 Geophysica aircraft, Borrmann et al. (2010) found that the aerosol number concentration, in average, over the lower stratosphere, is ranging from 40 to 100 particles per cm^3 for sizes greater than 10 nm in the tropical/subtropical region during the background period. Although the LOAC size lower bound is limited to 200 nm excluding the detection of the smallest particles, the observed concentrations on 19 May 2015 are above the levels recorded by the aircraft pointing out the impact of the Calbuco eruption on the lower stratospheric aerosol content. Three months later, another LOAC OPC was launched over the Reunion site but the in situ profile partially shows the volcanic aerosol layer because of a telemetry loss. The aerosol number concentration obtained on 19 August 2015 at 1300 UTC over Reunion may reveal a tendency to return to concentration values observed before the eruption (Fig. 9), with a number concentration of 40 particles per cm^3 in the lower stratosphere. This tendency is

confirmed with the LOAC flight conducted on 2 November 2016 at 2030 UTC with a total number concentration close to 20 particles per cm^3 in the lower stratosphere (Fig. 9).

The residence time of the aerosol particles in the stratosphere depends on the balance between the growth processes and the removal processes which are likely to be controlled by the dynamical context. In the following section, we will discuss the influence of the dynamical activity on the variability of the volcanic aerosol over the southern hemisphere.

4. Dynamical modulation of the aerosol plume

4.1 Long-range isentropic transport

In order to analyze the isentropic transport, the high resolution MIMOSA model has been used to produce a continuous evolution of PV fields for the period from 1 April 2015 to 31 August 2015. Four advected PV maps, derived for the 400 K isentropic level from the MIMOSA model, together with dynamical barrier locations derived from the DyBaL code are superimposed in Figures 10 and 11. The localization of the volcanic aerosol plume obtained from OMPS observations at 400 K ± 5 K isentropic level is also superimposed (Fig. 10 and 11). On 24 April 2015, a significant wave activity is observed, leading to a fairly mixed surf zone in the 20°S-60°S latitude band (not shown). The Calbuco plume is situated inside the surf zone and the plume was mixed equatorward. On 27 April 2015, the subtropical and mid-latitude barriers are detected following the Nakamura's formalism (described in Section 2.3) around 15°S and -40°S in latitude respectively, still limiting the geographical extent of the plume (Fig. 10a). Figure 10a shows clearly that the plume cannot move beyond the south of Brazil because of the presence of the subtropical barrier. On 01 May 2015, the air masses were confined between the two dynamical barriers located in average at 25°S and 40°S in latitude respectively. The air masses were advected eastward between South Africa and Madagascar following the wave shape of the barrier, in consistency with the OMPS observations near South Africa (Fig. 10b). The subtropical barrier previously located in average at 25°S moved northward crossing South Africa. The air masses containing aerosol previously situated in the south side of Madagascar were transported northward and eastward following the displacement of the barrier and reached the Reunion site.

On 19 May 2015, we note the presence of the subtropical and mid-latitude barriers around 28°S and 43°S respectively. (Fig. 11a). As expected, the volcanic aerosol plume was confined between the two dynamical barriers and embedded eastward. At this stage, the presence of the subtropical barrier and the polar vortex seems to drive significantly the Calbuco plume

inducing its transport eastward. Between end of May and beginning of June, the subtropical barrier has dissipated while the polar vortex was around ~40°S (see Fig. 11b). The OMPS observations reveal that the most part of the plume was located over the southern African and the Indian Ocean region in June (Fig. 11b). On the following months of July and August, the polar vortex is clearly identified at 60° S which is a classical pattern for the austral winter.

4.2 Removal processes

As shown above, in the lower stratosphere distributions of the aerosol are modulated (or mostly driven) by isentropic transport. However, particle removal processes should be considered. Based on a semi-Lagrangian transport model, Chen et al. (1994) showed that isentropic mass exchange between tropical and extratropical latitudes in the stratosphere can act as a significant removal process of stratospheric aerosols. Depending on the strength of the Brewer-Dobson circulation, stratospheric materials such as aerosols can be rapidly transported from the tropics to high latitudes (Dhomse et al., 2006, 2014).

Dhomse et al. (2014) using the CCM model (UM-UKCA) have revealed the influence of STE events on the budget of the stratospheric aerosols. In particular, they showed that overestimation of the strength of a STE event could lead to fast removal of aerosols from stratosphere into the middle and high latitude. Moreover, Hamill et al. (1997) reported that STE through the isentropic surfaces due to Rossby wave activity can be considered as a significant dynamical process for removal of stratospheric aerosol. Sixteen years of ozone measurements (1992–2006) at Reunion have been processed to detect stratospheric signatures on each single ozone profile by Clain et al. (2010). They shown that the STE occured frequently all the year at Reunion and strongly linked to dynamical processes occured near to tropopause such as tropopause fold. Given the potential of a STE event to impact the stratospheric aerosol loading, we cannot exclude its contribution (even though small) on the stratospheric aerosols loading at Reunion.

The modulation of the plume over Reunion could be also caused by particle removal processes such sedimentation which is considered as the primary loss mechanism of stratospheric aerosol or by dilution of the stratospheric plume (Hamill et al, 1997; Rasch et al., 2008). Nevertheless, the sedimentation of aerosol is an effective removal mechanism for the few particles that somehow survive long enough in the stratosphere to grow to larger sizes (Hamill et al., 1997). We note also that larger particles fall faster, which causes a vertical gradient in the particle size distribution (Mann et al., 2015). However, highlighting

sedimentation processes from Figures 6 and 7 is somewhat complicated by the transient feature of the volcanic aerosols with variable plume altitudes especially from the lidar local data.

5. Summary and conclusion

The long-range isentropic transport of the volcanic aerosol produced following the Calbuco eruption was examined. The analysis focuses on the dynamical context which led to the spread of the aerosol plume over Indian Ocean between April 2015 and November 2016. The transport of the volcanic aerosols to the Indian Ocean was investigated by combining satellite (CALIOP, IASI, OMPS), and ground-based experiments: Optical Particle Counter (LOAC) and lidar, in addition to numerical tools: the DyBal code and the high resolution MIMOSA model.

From the IASI observations, the amounts of SO_2 injected into the atmosphere during the Calbuco eruption have been quantified. SO_2 amounts emitted by the Calbuco eruption were about two times lower than for the Sarychev moderate eruption in the northern hemisphere in June 2009, but we report the same e-folding time for both eruptions, i.e. ~11 days (Jégou et al., 2013; Kravitz et al., 2011). It is found from CALIOP observations that the Calbuco aerosol layer was observable up to lower stratosphere, between 18 and 21 km, and spreaded exclusively over the Southern Hemisphere. Moreover, OMPS observations reveal that the Calbuco plume reached the Indian Ocean two weeks after the eruption. It is shown from ground-based observations deployed at Reunion Island that SAOD increased by a factor of ~2 by the beginning of May 2015 and decreased afterward and returned to pre-eruption values by November 2016. The aerosol e-folding time is estimated to be ~90 days, i.e. close to the ~80 days reported for the Sarychev eruption (Jégou et al., 2013). Though the various datasets rather agree in terms of aerosol signal intensity we report significant differences for the plume height and its variability possibly as a result of different observations geometries, resolutions and spatial scales inherent to each instrument.

In situ measurements by the LOAC OPC have pointed out the impact of the Calbuco eruption on the lower stratospheric aerosol content over the Reunion site. Aerosol number concentrations were 20 times higher than values observed before and one year after the eruption. On May 2015, the volcanic aerosol was characterized by an effective radius of 0.16 ±0.02 µm and an unimodal lognormal size distribution. These microphysical characteristics

are in agreement with previous studies focussing on the Sarychev eruption (Kravitz et al., 2011; Jégou et al., 2013).

Through the use of the MIMOSA model and the DyBAL code, it was clearly identified that the transport of the volcanic aerosols was eastward mainly in form of planetary-scale tongues. In particular, the combination of MIMOSA and DyBal simulations revealed that the transport of the volcanic aerosol plume eastward was controlled and confined between the subtropical barrier and polar vortex. The two dynamical barriers acted as a channel within which most of zonal transport took place, including transport of Calbuco plume. Our results support the assumption that the processes explaining the structure of the plume over the southern hemisphere had mainly a dynamical origin. Thus, the fluctuation of the localization of the dynamical barrier induced transient aerosol layers above Reunion and an inhomogeneous distribution of the plume between May and July 2015. The present study supports also the assumption that the modulation of a volcanic plume may result from the contribution of both dynamical and microphysical processes. Fully understanding the contribution of the microphysical processes on the evolution of the volcanic plume over the southern hemisphere requires further investigation. This will be examined in a forthcoming study.

Acknowledgements

This work is supported by the Labex « Étude des géofluides et des VOLatils–Terre, Atmosphère et Interfaces - Ressources et Environnement (VOLTAIRE) (ANR-10-LABX-100-01). This study is integrated and supported by the LEFE project SATORI (Stratospheric Aerosols in the Tropic Observed from Reunion Island). The authors thank the LPC2E and UMS balloon launching team for their technical collaboration. We would especially like to thank the staff of the team working on the lidar systems at the Maïdo observatory. Lieven Clarisse is a research associate with the Belgian FNRS-F.R.S. The authors thank also the CALIOP team and Jean-Paul Vernier for processing and providing data. We are also grateful to the CCUR team for the use of the TITAN supercomputer.

References

Arfeuille, F., B. P. Luo, P. Heckendorn, D. Weisenstein, J. X. Sheng, E. Rozanov, M. Schraner, S. Brönnimann, L.W. Thomason, and T. Peter: Modeling the stratospheric warming following the Mt. Pinatubo eruption: uncertainties in aerosol extinctions, Atmos. Chem. Phys., 13, 11221–11234, 2013.

Baray, J. L., Courcoux, Y., Keckhut, P., Portafaix, T., Tulet, P., Cammas, J. P., ... & Desmet, F. (2013). Maïdo observatory: a new high-altitude station facility at Reunion Island (21° S, 55° E) for long-term atmospheric remote sensing and in situ measurements. *Atmospheric Measurement Techniques*, *6*(10), 2865-2877.

Bauman, J. J., Russell, P. B., Geller, M. A. and Hamill, P. : A stratospheric aerosol climatology from SAGE II and CLAES measurements: 2. Results and comparisons, 1984–1999. J. Geophys.Res. 108, 4383. (doi:10.1029/2002JD002993, 2003

Bekki, S : On the possible role of aircraft-generated soot in the middle latitude ozone depletion, *J. Geophys. Res.*, *102*, 10,751-10,758, 1997

Bencherif, H., Portafaix, T., Baray, J. L., Morel, B., Baldy, S., Leveau and J., Diab, R. : LIDAR observations of lower stratospheric aerosols over South Africa linked to large scale transport across the southern subtropical barrier. *Journal of atmospheric and solar-terrestrial physics*, *65*(6), 707-715, 2003

Bencherif, H., Amraoui, L. E., Semane, N., Massart, S., Charyulu, D. V., Hauchecorne, A., and Peuch, V. H., Examination of the 2002 major warming in the southern hemisphere using ground-based and Odin/SMR assimilated data: stratospheric ozone distributions and tropic/mid-latitude exchange. *Canadian Journal of Physics*, *85*(11), 1287-1300, 2007

Bluth, G. J. S., Doiron, S. D., Schnetzler, C. C., Krueger, A. J., and Walter, L. S.: Global tracking of the SO2 clouds from the June 1991 Mount Pinatubo eruptions, Geophys. Res. Lett., 19, 151–154, doi:10.1029/91GL02792, 1992.

Borrmann, S., Solomon, S., Dye, J. E., Baumgardner, D., Kelly, K.K., and Chan, K. R.: Heterogeneous reactions on stratospheric background aerosols, volcanic sulfuric acid droplets, and type I PSCs: The effects of temperature fluctuations and differences in particle phase, J. Geophys. Res., 102, 3639–3648, 1997.

Bourassa, A. E., D. A. Degenstein, B. J. Elash, and E. J. Llewellyn : Evolution of the stratospheric aerosol enhancement following the eruptions of Okmok and Kasatochi:

Odin-OSIRIS measurements, J. Geophys.Res., 115, D00L03, doi:10.1029/2009JD013274, 2010

Bourassa, A. E., McLinden, C. A., Bathgate, A. F., Elash,B. J., and Degenstein, D. A.: Precision estimate for Odin-OSIRIS limb scatter retrievals, J. Geophys. Res., 117, D04303, doi:10.1029/2011JD016976, 2012

Canty, T., Mascioli, N. R., Smarte, M. D., & Salawitch, R. J. (2013). An empirical model of global climate-Part 1: A critical evaluation of volcanic cooling. *Atmospheric Chemistry and Physics*, *13*(8), 3997.

Carn, S., L. Clarisse, and A. J. Prata : Multi-decadal satellite measurements of global volcanic degassing, J. Volcanol. Geotherm. Res., 99-134, 2016

Chen, P., J. R. Holton, A. O'Neill, and R. Swinbank, 1994: Isentropic mass exchange between the Tropics and extratropics in the stratosphere. *J. Atmos. Sci.*, **51,** 3006–3018.

Clain, G., Baray, J. L., Delmas, R., Keckhut, P and Cammas, J. P : A lagrangian approach to analyse the tropospheric ozone climatology in the tropics: Climatology of stratosphere–troposphere exchange at Reunion Island. *Atmospheric environment*, *44*(7), 968-975, 2010

Clarisse, L., Coheur, P. F., Prata, A. J., Hurtmans, D., Razavi, A., Phulpin, T., Hadji-Lazaro, J., and Clerbaux, C.: Tracking and quantifying volcanic SO2 with IASI, the September 2007 eruption at Jebel at Tair, Atmos. Chem. Phys., 8, 7723-7734, doi:10.5194/acp-8-7723-2008, 2008.

Clarisse, L., Hurtmans, D., Clerbaux, C., Hadji-Lazaro, J., Ngadi,Y., and Coheur, P.-F.: Retrieval of sulphur dioxide from the infrared atmospheric sounding interferometer (IASI), Atmos. Meas. Tech., 5, 581–594, doi:10.5194/amt-5-581-2012, 2012.

Clarisse, L., Coheur, P. F., Theys, N., Hurtmans, D. and Clerbaux, C.: The 2011 Nabro eruption, a SO_2 plume height analysis using IASI measurements. *Atmospheric chemistry and physics*, *14*(6), 3095-3111, 2014

Clerbaux, C., Boynard, A., Clarisse, L., George, M., Hadji-Lazaro, J., Herbin, H. and Wespes, C. Monitoring of atmospheric composition using the thermal infrared IASI/MetOp sounder. *Atmospheric Chemistry and Physics*, *9*(16), 6041-6054, 2009

Dhomse, S., Weber, M., Wohltmann, I., Rex, M.,and Burrows, J. P.,. On the possible causes of recent increases in northern hemispheric total ozone from a statistical analysis of satellite data from 1979 to 2003. *Atmospheric Chemistry and Physics*, *6*(5), 1165-1180, 2006

Dhomse, S. S., Emmerson, K. M., Mann, G. W., Bellouin, N., Carslaw, K. S., Chipperfield, M. P. and Dalvi, M. , Aerosol microphysics simulations of the Mt.~ Pinatubo eruption with the UM-UKCA composition-climate model. *Atmospheric Chemistry and Physics*, *14*(20), 11221-11246, 2014

Fairlie, T. D., J. P. Vernier, M. Natarajan, and K. M. Bedka (2014), Dispersion of the Nabro volcanic plume and its relation to the Asian summer monsoon, Atmos. Chem. Phys., 14(13), 7045-7057, doi:10.5194/acp-14-7045-2014.

Froyd, K. D., D. M. Murphy, T. J. Sanford, D. S. Thomson, J. C. Wilson, L. Pfister, and L. Lait : Aerosol composition of the tropical upper troposphere, Atmos. Chem. Phys., 9, 4363-4385, 2009

Fussen, D., F. Vanhellemont and C. Bingen, Evidence of transport, sedimentation and coagulation mechanisms in the relaxation of post-volcanic stratospheric aerosols, *Ann. Geophys.*, *19*, 1157-1162, 2001

Gorkavyi, N., D. F. Rault, P. A. Newman, A. M. d. Silva, and A. E. Dudorov : New stratospheric dust belt due to the Chelyabinsk bolide, Geophys. Res. Lett., 40(17), 47284733, doi:10.1002/grl.50788, 2013

Grant, W. B., Browell, E. V., Fishman, J., Brackett, V. G., Veiga, R. E., Nganga, D., .Long, C. S. : Aerosol-associated changes in tropical stratospheric ozone following the eruption of Mount Pinatubo. *Journal of Geophysical Research: Atmospheres*, *99*(D4), 8197-8211, 1994

Grant, W. B., E. V. Browell, C. S. Long, L. L. Stowe, R. G.Grainger, and A. Lambert : Use of volcanic aerosols to study the tropical stratospheric reservoir. *J. Geophys. Res.*, **101,**3973–3988, 1996

Hauchecorne, A., Godin, S., Marchand, M., Heese, B., and Souprayen, C. Quantification of the transport of chemical constituents from the polar vortex to midlatitudes in the lower stratosphere using the high-resolution advection model MIMOSA and effective diffusivity. *Journal of Geophysical Research: Atmospheres*, *107*(D20), 2002

Heese, B., Godin, S and Hauchecorne, A : Airborne lidar measurements of ozone filaments during METRO–A validation of PV advection model MIMOSA. *J. Geophys. Res*, *106*, 20-011, 2001

Hommel, R., Timmreck, C., Giorgetta, M. A. and Graf, H. F. (2015). Quasi-biennial oscillation of the tropical stratospheric aerosol layer. *Atmospheric Chemistry and Physics*, *15*(10), 5557, 2015

Jaross, G., Chen, G., Kowitt, M., Warmer, J;, Xu, P., Kelly, T. and Flittner, D : Suomi NPP OMPS Limb Profiler initial sensor performance assessment. In SPIE asia-Pacific Remote Sensing (pp. 852805-852805), International Society for Optics and Photonics, 2012

Junge, C. E., Chagnon, C. W., & Manson, J. E. (1961). Stratospheric aerosols. *Journal of Meteorology*, *18*(1), 81-108.

Kinnison, D. E., K. E. Grant, P. S. Connell, D. A. Rotman, *and* D. J. Wuebbles *(*1994*),* The chemical and radiative effects of the Mount Pinatubo eruption, J. Geophys. Res., 99*(*D12*),* 25705–25731, *doi:*10.1029/94JD02318.

Klett, J. D : Stable analytical inversion solution for processing lidar returns, Appl. Opt., 20, 211 – 220, 1981

Kravitz, B., Robock, A., and Bourassa, A.: Negligible climatic effects from the 2008 Okmok and Kasatochi volcanic eruptions,J. Geophys. Res., 115, D00L05, oi:10.1029/2009JD013525, 2010.

Kravitz, B., Robock, A., Bourassa, A., Deshler, T., Wu, D., Mattis, I., Finger, F., Hoffmann, A., Ritter, C., Bitar, L., Duck, T. J.,and Barnes, J. E.: Simulation and observations of stratospheric aerosols from the 2009 Sarychev volcanic eruption, J. Geophys.Res., 116, D18211, doi:10.1029/2010JD015501, 2011.

Kravitz, B., Robock, A., Shindell, D. T. and Miller, M. A.. Sensitivity of stratospheric geoengineering with black carbon to aerosol size and altitude of injection. *Journal of Geophysical Research: Atmospheres*, *117*(D9), 2002

Kremser, S., Thomason, L. W., Hobe, M., *et al.* Stratospheric aerosol—Observations, processes, and impact on climate. *Reviews of Geophysics*, vol. 54, no 2, p. 278-335, 2016

Hamill, P., Jensen, E. J., Russell, P. B., and Bauman, J.J.: The life cycle of stratospheric aerosol particles, B.Am. Meteorol. Soc., 78, 1395–1410, doi:10.1175/1520-0477(1997)078<1395:TLCOSA>2.0.CO;2, 1997.

Krotkov, N. A., M. R. Schoeberl, G. A. Morris, S. Carn, and K. Yang : Dispersion and lifetime of the SO2 cloud from the August 2008 Kasatochi eruption, J. Geophys. Res., 115, doi:10.1029/2010jd013984, 2010

Hermann, M., J. Heintzenberg, A. Wiedensohler, A. Zahn, G. Heinrich, and C. A. M. Brenninkmeijer, Meridional distributions of aerosol particle number concentrations in the upper troposphere and lower stratosphere obtained by Civil Aircraft for Regular Investigation of the Atmosphere Based on an Instrument Container (CARIBIC) flights, J. Geophys. Res., 108(D3), 4114, doi:10.1029/2001JD001077, 2003.

Hofmann, D., Barnes, J., O'Neill, M., Trudeau, M., and Neely, R.:Increase in background stratospheric aerosol observed with lidar at Mauna Loa Observatory and Boulder, Colorado, Geophys.Res. Lett., 36, L15808, doi:10.1029/2009GL039008, 2009.

Hitchman, M. H., M. McKay and C. R. Trepte (1994), A climatology of stratospheric aerosol, *J. Geophys. Res.*, *99*, 20,689-20,700.

Jäger, H., and T. Deshler, Lidar backscatter to extinction, mass and area conversions for stratospheric aerosols based on midlatitude balloonborne size distribution measurements,Geophys. Res. Lett., 29(19), 1929, doi:10.1029/2002GL015609, 2002.

Jégou, F., Berthet, G., Brogniez, C., Renard, J. B., François, P., Haywood, J. M. and Godin-Beekmann, S. (2013). Stratospheric aerosols from the Sarychev volcano eruption in the 2009 Arctic summer. *Atmospheric Chemistry and Physics*, *13*(13), 6533-6552.

Labitzke, K. and McCormick, M.: Stratospheric temperature increases due to Pinatubo aerosols, Geophys. Res. Lett., 19, 207–210, 1992.

Lurton, T., Renard, J.-B., Vignelles, D., Jeannot, M., Akiki, R., Mineau, J.-L. and Tonnelier, T.: Light scattering at small angles by atmospheric irregular particles: modelling and laboratory measurements, Atmos., Meas. Tech., 7, 931-939, 2014.

McCormick, M. P., Thomason, L. W., and Trepte, C. R.: Atmospheric effects of the Mt Pinatubo eruption, Nature, 373, 399–404, 1995.

Morel, B., Bencherif, H., Keckhut, P., Portafaix, T., Hauchecorne, A., and Baldy, S., Fine-scale study of a thick stratospheric ozone lamina at the edge of the southern subtropical barrier: 2. Numerical simulations with coupled dynamics models. *Journal of Geophysical Research: Atmospheres*, *110*(D17), 2005

Nakamura, N., Two-dimensional mixing, edge formation, and permeability diagnosed in an area coordinate. *Journal of the atmospheric sciences*, *53*(11), 1524-1537, 1996

Neely, R. R., P. Yu, K. H. Rosenlof, O. B. Toon, J. S. Daniel, S. Solomon, and H. L. Miller (2014), The contribution of anthropogenic SO2emissions to the Asian tropopause aerosol layer, J. Geophys. Res., 119(3), 1571-1579, doi:10.1002/2013JD020578.

O'Neill, N. T., Perro, C., Saha, A., Lesins, G., Duck, T. J., Eloranta, E. W and Bourassa, A : Properties of Sarychev sulphate aerosols over the Arctic. *Journal of Geophysical Research: Atmospheres*, *117*(D4), 2012

Portafaix, T., Morel, B., Bencherif, H., Baldy, S., Godin-Beekmann, S., and Hauchecorne, A.. Fine-scale study of a thick stratospheric ozone lamina at the edge of the southern subtropical barrier. *Journal of Geophysical Research: Atmospheres*, *108*(D6), 2003

Pueschel, R. F., Snetsinger, K. G., Russell, P. B., Kinne, S. A., & Livingston, J. M : The effects of the 1991 Pinatubo volcanic eruption on the optical and physical properties of stratospheric aerosols. *Proceedings of IRS92: Current Problems in Atmospheric Radiation*, 183-186, 1992

Rasch, P. J., Tilmes, S., Turco, R. P., Robock, A., Oman, L., Chen, C. C. J. and Garcia, R. R., An overview of geoengineering of climate using stratospheric sulphate aerosols. *Philosophical Transactions of the Royal Society of London A: Mathematical, Physical and Engineering Sciences*, *366*(1882), 4007-4037, 2008

Randel, W. J., Gille, J. C., Roche, A. E., Kumer, J. B., Mergenthaler, J. L., Waters, J. W. and Lahoz, W. A. (1993). Stratospheric transport from the tropics to middle latitudes by planetary-wave mixing. *Nature*, *365*(6446), 533-535.

Rault, D.F and Loughmann,R.P : The OMPS Limb Profiler environmental data record algorithm theoretical basis document and expected performance, IEEE Transactions on Geoscience and Remote Sensing, 51(5), 2505-2527, 2013

Renard, J.B., Dulac, F., Berthet, G., Lurton, T., Vignelles, D., Jégou, F., Tonnelier, T., Thaury, C., Jeannot, M., Couté, B., Akiki, R., Verdier, N., Mallet, M., Gensdarmes, F., Charpentier, P., Duverger, V., Dupont, J.V., Mesmin, S., Elias, T., Crenn, V., Sciare, J., Giacomoni, J., Gobbi, M., Hamonou, E., Olafsson, H., Dagsson-Waldhauserova, P., Camy-Peyret, C., Mazel, C., Décamps, T., Piringer, M., Surcin, J., and Daugeron, D.: LOAC: a small aerosol optical counter/sizer for ground-based and balloon measurements of the size

distribution and nature of atmospheric particles – Part 1: Principle of measurements and intercomparison campaigns, *Atmos. Meas. Tech.*, 9, 1721–1742, doi:10.5194/amt-9-1721-2016, 2016.

Ridley, D. A., et al. : Total volcanic stratospheric aerosol optical depths and implications for global climate change, Geophys. Res. Lett., 41(22), 7763-7769, doi:10.1002/2014GL061541, 2014

Russell, P. B., Livingston, J. M., Pueschel, R. F., Bauman, J. J., Pollack, J. B., Brooks, S. L. and Dutton, E. G. (1996). Global to microscale evolution of the Pinatubo volcanic aerosol derived from diverse measurements and analyses. *Journal of Geophysical Research: Atmospheres*, *101*(D13), 18745-18763.

Sasano, Y., Browell, E. V. and Ismail, S : Error caused by using a constant extinction/backscattering ratio in the lidar solution. *Applied Optics*, *24*(22), 3929-3932, 1985

Sawamura, P., Vernier, J. P., Barnes, J. E., Berkoff, T. A., Welton, E. J., Alados-Arboledas, L. and Lange, D. (2012). Stratospheric AOD after the 2011 eruption of Nabro volcano measured by lidars over the Northern Hemisphere. *Environmental Research Letters*, *7*(3), 034013.

Siddaway, J. M., and S. V. Petelina (2010), Transport and evolution of the 2009 Australian Black Saturday bushfire smoke in the lower stratosphere observed by OSIRIS on Odin, J. Geophys. Res., 116, doi:10.1029/2010JD015162.

Solomon, S., Portmann, R. W., Garcia, R. R., Thomason, L. W.,Poole, L. R., and McCormick, M. P.: The role of aerosol variations in anthropogenic ozone depletion at northern midlatitudes, J. Geophys. Res.-Atmos., 101, 6713–6727, 1996.

Solomon, S., Stratospheric ozone depletion: A review of concepts and history, Rev. Geophys., 37, 275–316, doi:10.1029/1999RG900008, 1999

Solomon, S., Daniel, J. S., Neely III, R. R., Vernier, J.-P., Dutton, E. G., and Thomason, L. W.: The persistently variable ”Background”stratospheric aerosol layer and global climate change,Science 333, 866, doi:10.1126/science.1206027, 2011.

SPARC 2006 Assessment of stratospheric aerosol properties (ASAP). Technical report WCRP-124/WMO/TD-No. 1295/SPARC report no. 4, SPARC, Toronto, Ontario, CA, pp. 322.

Stenchikov, G. L., Kirchner, I., Robock, A., Graf, H. F., Antuna, J. C., Grainger, R. G., Lambert, A. & Thomason, L. 1998 Radiative forcing from the 1991 Mount Pinatubo volcanic eruption conditions. J. Geophys. Res. 103, 13 837–13 857. (doi:10.1029/98JD00693)

Stenchikov, G., A. Robock, V. Ramaswamy, M. D. Schwarzkopf, K. Hamilton, *and* S. Ramachandran, Arctic Oscillation response to the 1991 Mount Pinatubo eruption: Effects of volcanic aerosols and ozone depletion, J. Geophys. Res., 107*(*D24*)*, *4803*, *doi:*10.1029/2002JD002090, 2002.

Schuster, G. L., O. Dubovik, and B. N. Holben : Angstrom exponent and bimodal aerosol size distributions, J. Geophys. Res., 111, D07207, doi:10.1029/2005JD006328, 2006

Thomason, L. W., Pitts, M. C., & Winker, D. M. (2007). CALIPSO observations of stratospheric aerosols: a preliminary assessment. *Atmospheric Chemistry and Physics*, *7*(20), 5283-5290.

Thomason, L. W., S. P. Burton, B.-P. Luo and T. Peter , SAGE II measurements of stratospheric aerosol properties at non-volcanic levels, *Atmos.* Chem. *Phys.*, *8*, 983-995, 2008

Trepte, C. R., and Hitchman, M. H.: Tropical stratospheric circulation deduced from satellite aerosol data, Nature, Vol. 355, 626-628, 1992.

Trepte, C. R., Veiga, R. E., and McCormick, M. P. : The poleward dispersal of Mount Pinatubo volcanic aerosol, J. Geophys. Res., vol. 98, No. D10, 18,563-18,573, 1993.

Vernier, J. P., Pommereau, J. P., Garnier, A., Pelon, J., Larsen, N., Nielsen, J., and McDermid, I. S., Tropical stratospheric aerosol layer from CALIPSO lidar observations. *Journal of Geophysical Research: Atmospheres*, *114*(D4), 2009

Vernier, J.-P., Thomason, L. W., Pommereau, J.-P., Bourassa, A.,Pelon, J., Garnier, A., Hauchecorne, A., Blanot, L., Trepte,C., Degenstein, D., and Vargas, F.: Major influence of tropical volcanic eruptions on the stratospheric aerosol layer during the last decade, Geophys. Res. Lett., 38, L12807,doi:10.1029/2011GL047563, 2011.

Winker, D., Vaughan, M., Omar, A., Hu, Y., Powell, K., Liu, Z., Hunt, Wand Young, S : Overview of the calipso mission and caliop data processing algorithms, *J. Atmos.*1139 *Oceanic Technol.*, *26*, 2310–2323, 2009

Vignelles, D. : Caractérisation des performances du nouveau mini compteur de particule LOAC embarqué sous ballon météorologique : application à l'étude de la variabilité spatiale

et temporelle des aérosols de la haute troposphère et de la stratosphère - PhD Thesis, Univ. Orléans, 2016

Weigel, R., Hermann, M., Curtius, J., Voigt, C., Walter, S., Böttger, T and Borrmann, S : Experimental characterization of the COndensation PArticle counting System for high altitude aircraft-borne application. *Atmospheric Measurement Techniques*, *2*, 243-258, 2009

Wunderlich, F. and Mitchell, D. M : Revisiting the observed surface climate response to large volcanic eruptions. *Atmospheric Chemistry and Physics*, *17*(1), 485-499, 2017

Xu, W., Jónsson, S., Ruch, J. and Aoki, Y : The 2015 Wolf volcano (Galápagos) eruption studied using Sentinel-1 and ALOS-2 data. *Geophysical Research Letters*, *43*(18), 9573-9580, 2016

Atmos. Chem. Phys. Discuss., https://doi.org/10.5194/acp-2017-544
Manuscript under review for journal Atmos. Chem. Phys.
Discussion started: 22 June 2017

Atmospheric Chemistry and Physics Discussions

FIGURES AND TABLES

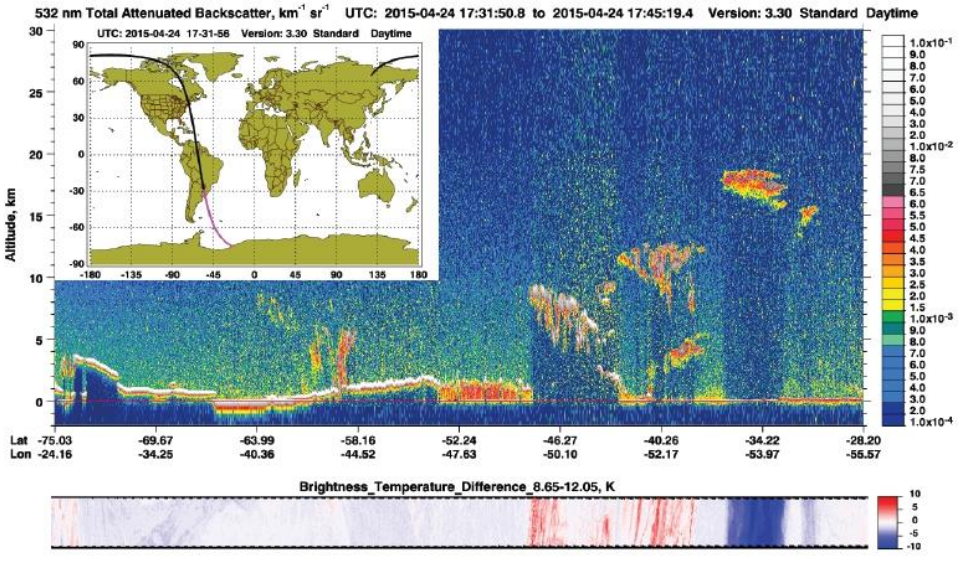

Figure 1 : CALIOP cross-section of 532 nm attenuated backscatter for the overpass at 1730-1745 on 24 April 2015.

Atmos. Chem. Phys. Discuss., https://doi.org/10.5194/acp-2017-544
Manuscript under review for journal Atmos. Chem. Phys.
Discussion started: 22 June 2017

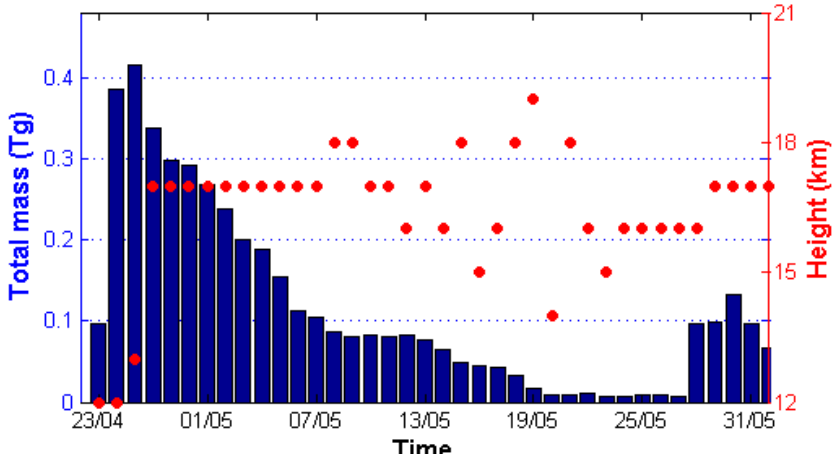

Figure 2 : Evolution of the SO_2 total mass (in blue) and the height of the maximum SO_2 mass obtained from IASI from 23 April 2015 to 31 May 2015 over the Southern Hemisphere.

Atmos. Chem. Phys. Discuss., https://doi.org/10.5194/acp-2017-544
Manuscript under review for journal Atmos. Chem. Phys.
Discussion started: 22 June 2017

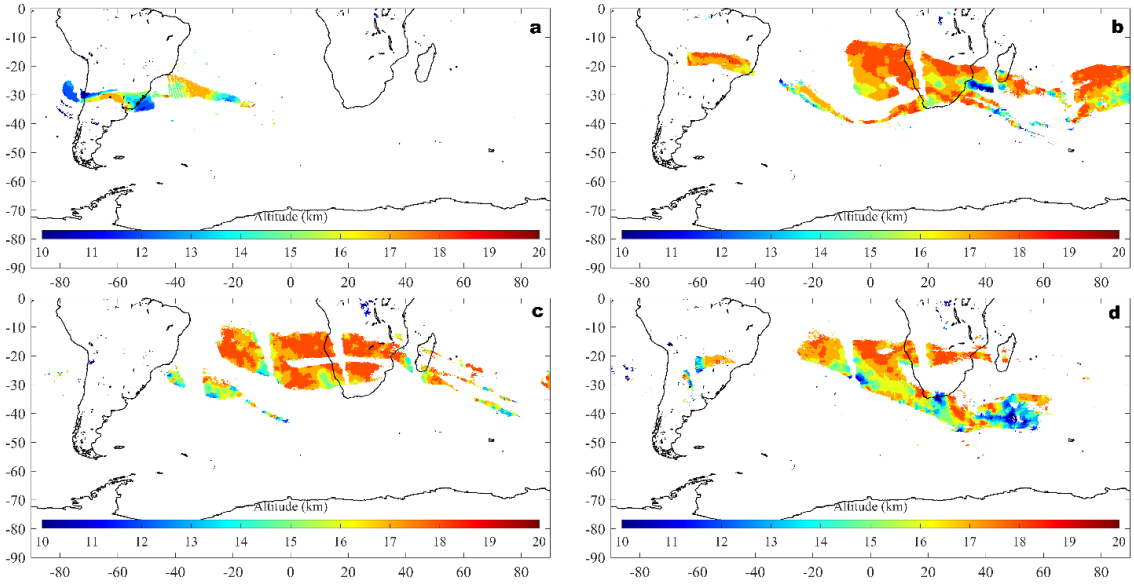

Figure 3 : *Height injection(in km) and transport of SO_2 obtained from IASI observations during (a) 24/04, (b) 01/05, (c) 06/05 and (d) 11/05*

Atmos. Chem. Phys. Discuss., https://doi.org/10.5194/acp-2017-544
Manuscript under review for journal Atmos. Chem. Phys.
Discussion started: 22 June 2017

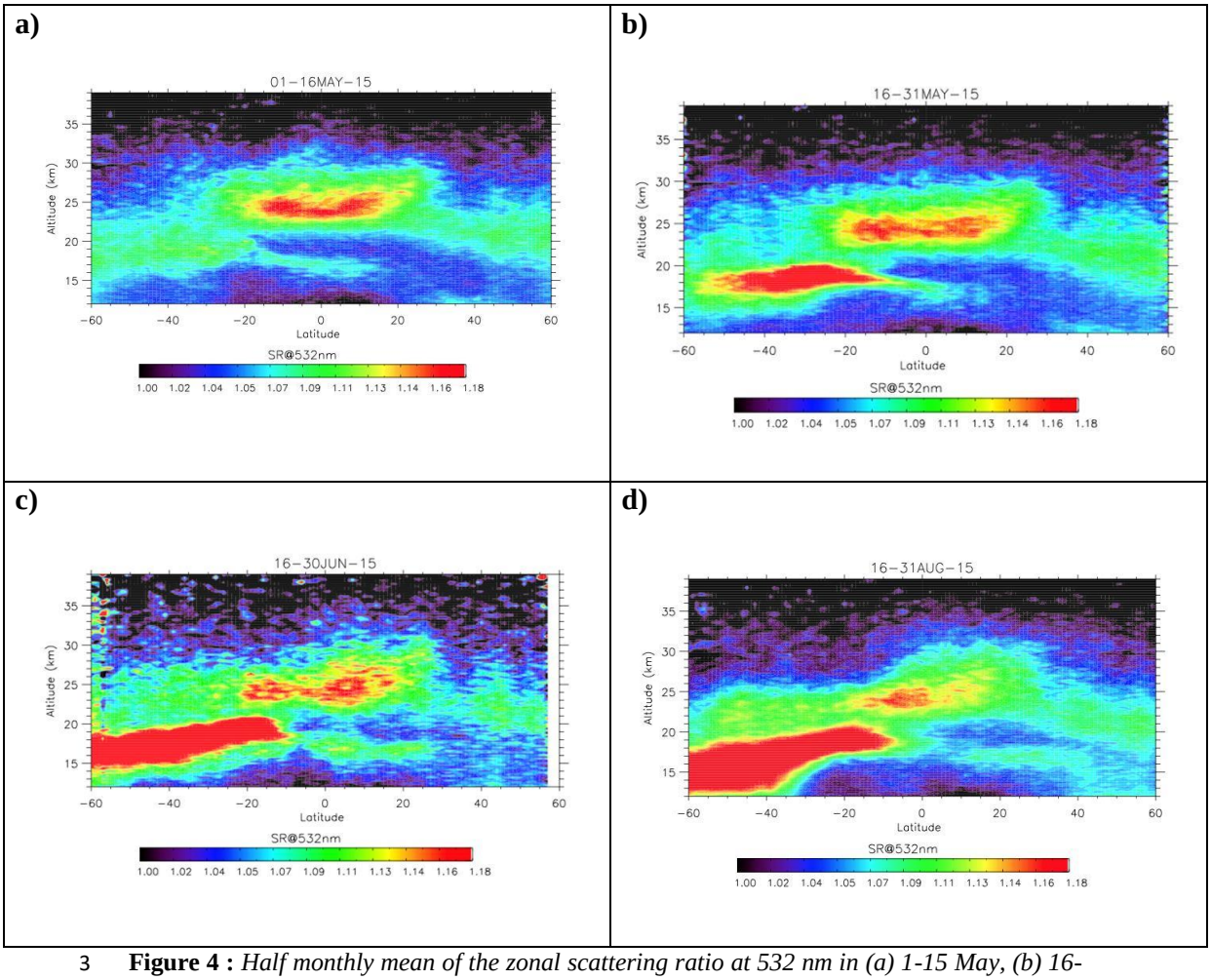

Figure 4 : *Half monthly mean of the zonal scattering ratio at 532 nm in (a) 1-15 May, (b) 16-31 May, (c) 16-30 June and (d) 16-31 August.*

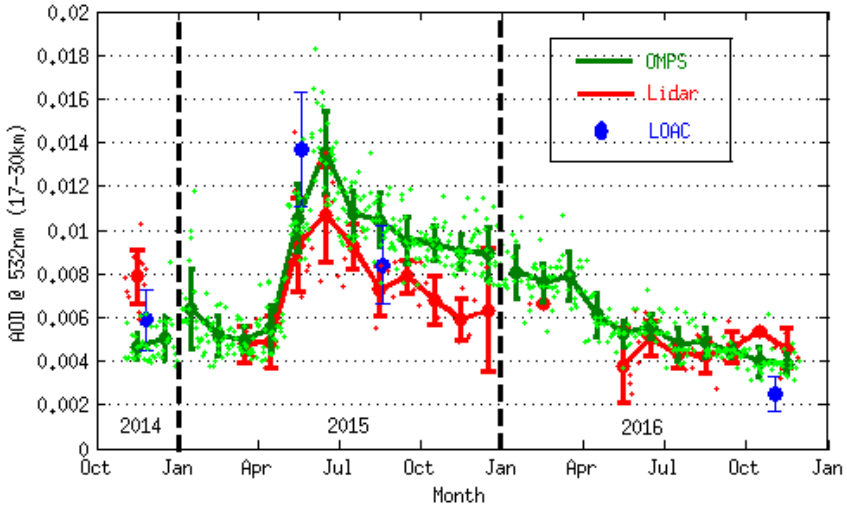

Figure 5 : *Evolution of AOD calculated between 17 and 30 km at 532 nm obtained from lidar (red), LOAC OPC (blue) and OMPS (green) observations between November 2014 to November 2016 over the Reunion site. The small dots represent the daily AOD and the large dots represent the monthly averaged AOD obtained from the devices.*

Atmos. Chem. Phys. Discuss., https://doi.org/10.5194/acp-2017-544
Manuscript under review for journal Atmos. Chem. Phys.
Discussion started: 22 June 2017

1

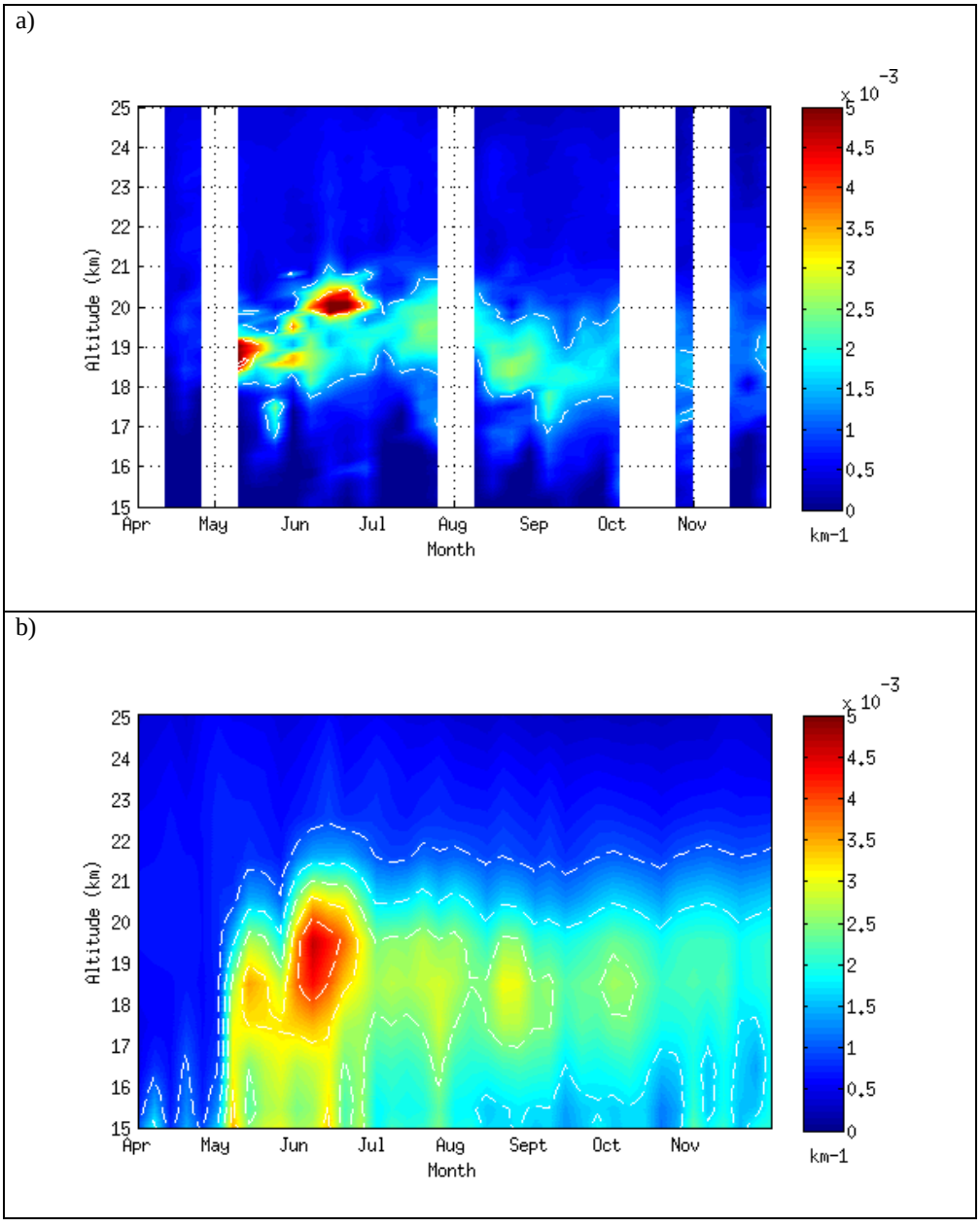

2 **Figure 6 :** Time series of weekly-averaged profiles of extinction at 532 nm obtained from (a)
3 lidar and (b) OMPS observations over Reunion between April 2015 and December 2015.

4

Atmos. Chem. Phys. Discuss., https://doi.org/10.5194/acp-2017-544
Manuscript under review for journal Atmos. Chem. Phys.
Discussion started: 22 June 2017

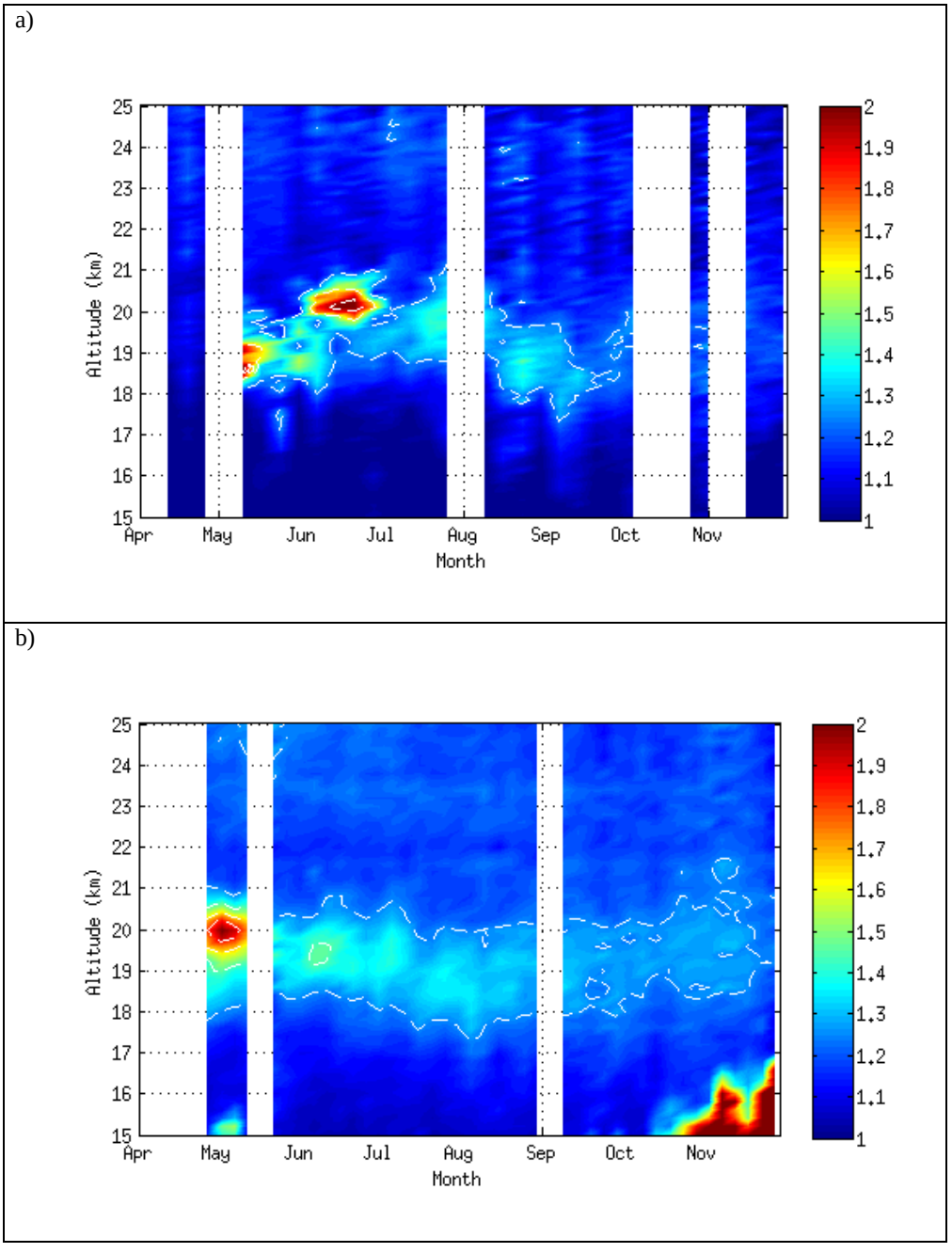

Figure 7 : Time series of *weekly-averaged profiles of scattering ratio at 532 nm obtained from (a) lidar and (b) CALIOP observations over Reunion between April 2015 and December 2015.*

Atmos. Chem. Phys. Discuss., https://doi.org/10.5194/acp-2017-544
Manuscript under review for journal Atmos. Chem. Phys.
Discussion started: 22 June 2017

Atmospheric Chemistry and Physics Discussions

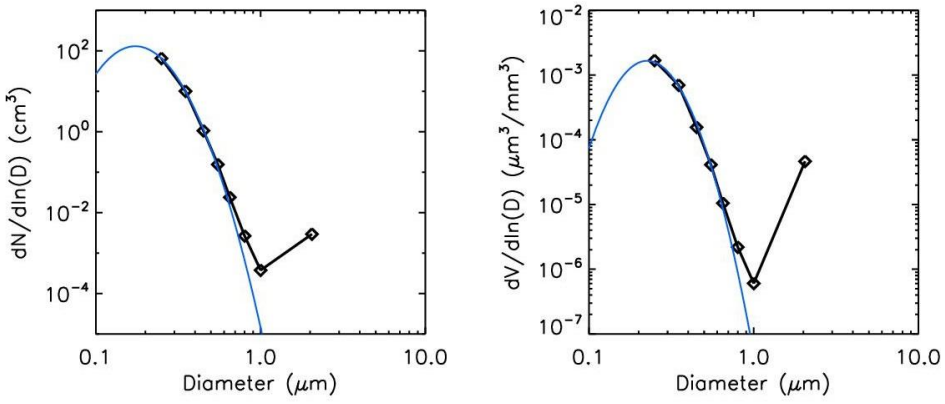

Figure 8 : Number (dN/dln(D)) and Volume concentration (dV/dln(D)) obtained from LOAC OPC observations on 19 May 2015 at 1746 UTC over the Reunion site.

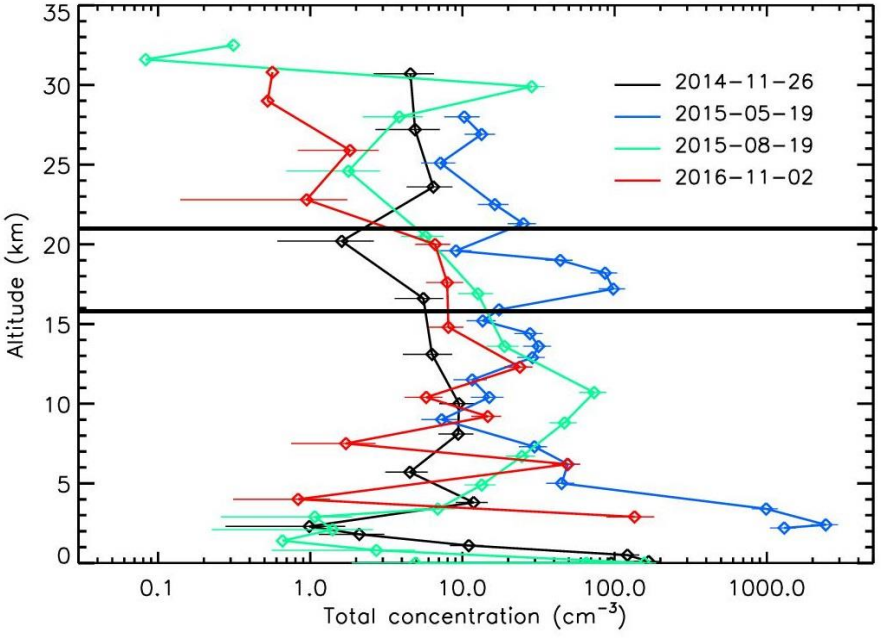

Figure 9 : Total number concentration of aerosols (0.2-50µm) profiles obtained from LOAC OPC observations over Reunion during the 26 November 2014 (black line), the 19 May 2015 (blue line), the 19 August 2015 (green line) and the 2 November 2016 (red line). The aerosols layer is delimited by two horizontal black lines.

Atmos. Chem. Phys. Discuss., https://doi.org/10.5194/acp-2017-544
Manuscript under review for journal Atmos. Chem. Phys.
Discussion started: 22 June 2017

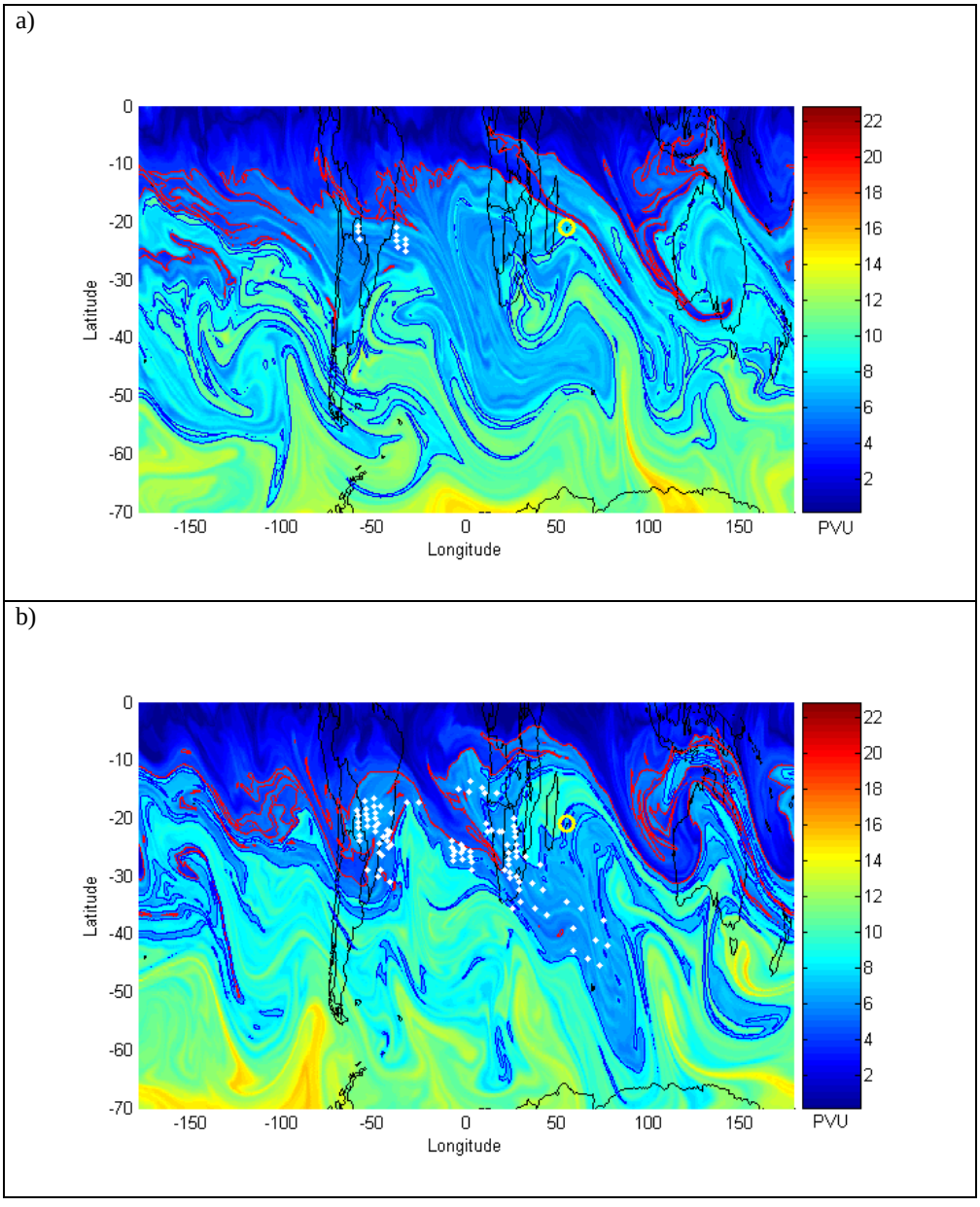

Figure 10 : Advected PV map at the 400 K level obtained from the MIMOSA model (a) on 27 April 2015 and (b) on 01 May 2015. The positions of the subtropical barrier (red line) and a south dynamical barrier (blue line) are detected from the DyBAL code. The white dots represent the localization of the aerosol plume at 400 K ± 5 K obtained from OMPS observations, while the yellow circles indicate the Reunion site.

Atmos. Chem. Phys. Discuss., https://doi.org/10.5194/acp-2017-544
Manuscript under review for journal Atmos. Chem. Phys.
Discussion started: 22 June 2017

Atmospheric Chemistry and Physics Discussions

1

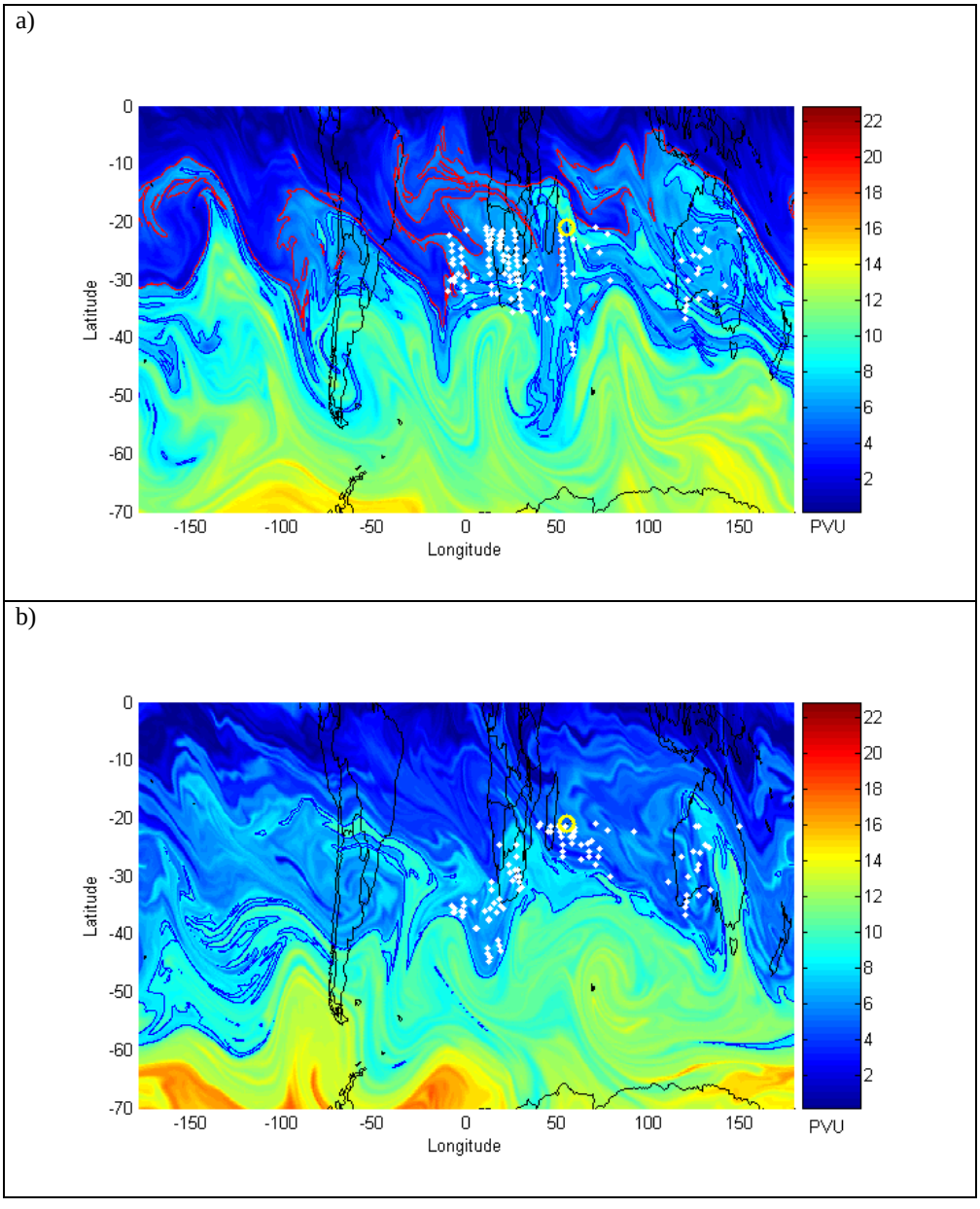

2 **Figure 11:** Same as Figure 10 but for (a) 19 May 2015 and (b) 03 June 2015.